LETTERS

Role for perinuclear chromosome tethering in maintenance of genome stability

Karim Mekhail[1,2], Jan Seebacher[2], Steven P. Gygi[2] & Danesh Moazed[1,2]

Repetitive DNA sequences, which constitute half the genome in some organisms, often undergo homologous recombination. This can instigate genomic instability resulting from a gain or loss of DNA[1]. Assembly of DNA into silent chromatin is generally thought to serve as a mechanism ensuring repeat stability by limiting access to the recombination machinery[2]. Consistent with this notion is the observation, in the budding yeast *Saccharomyces cerevisiae*, that stability of the highly repetitive ribosomal DNA (rDNA) sequences requires a Sir2-containing chromatin silencing complex that also inhibits transcription from foreign promoters and transposons inserted within the repeats by a process called rDNA silencing[2–5]. Here we describe a protein network that stabilizes rDNA repeats of budding yeast by means of interactions between rDNA-associated silencing proteins and two proteins of the inner nuclear membrane (INM). Deletion of either the INM or silencing proteins reduces perinuclear rDNA positioning, disrupts the nucleolus–nucleoplasm boundary, induces the formation of recombination foci, and destabilizes the repeats. In addition, artificial targeting of rDNA repeats to the INM suppresses the instability observed in cells lacking an rDNA-associated silencing protein that is typically required for peripheral tethering of the repeats. Moreover, in contrast to Sir2 and its associated nucleolar factors, the INM proteins are not required for rDNA silencing, indicating that Sir2-dependent silencing is not sufficient to inhibit recombination within the rDNA locus. These findings demonstrate a role for INM proteins in the perinuclear localization of chromosomes and show that tethering to the nuclear periphery is required for the stability of rDNA repeats. The INM proteins studied here are conserved and have been implicated in chromosome organization in metazoans[6,7]. Our results therefore reveal an ancient mechanism in which interactions between INM proteins and chromosomal proteins ensure genome stability.

Eukaryotic rDNA is tandemly repeated from about 100 to more than 10,000 times[8]. rDNA repeats provide the foundation for at least one ribosome-manufacturing compartment, the nucleolus. The budding yeast *Saccharomyces cerevisiae* has 100–200 rDNA units tandemly arranged on chromosome XII (Chr. XII) and forming one nucleolus (Fig. 1a, b)[8]. In addition to harbouring rRNA-coding DNA sequences, each unit contains intergenic spacers (IGS1 and IGS2) that promote repeat integrity (Fig. 1a)[9–11]. Recruitment of nucleolar protein complexes RENT (regulator of nucleolar silencing and telophase exit; composed of Cdc14, Net1/Cfi1 and Sir2) and Cohibin (mitotic monopolin proteins Lrs4 and Csm1) to IGS1 suppresses unequal recombination at the repeats[3,12–16]. This suppression is seemingly linked to the ability of these complexes to induce rDNA silencing, which involves chromatin changes preventing RNA polymerase II (Pol II)-driven transcription within IGSs of rDNA[4,5,16–19].

Purification of Cohibin suggested an association with INM proteins of unknown function[16]. To gain insight into the possible role of this association in nucleolar organization, we purified native Cohibin and INM proteins by tandem affinity purification (TAP). The TAP-tagged proteins are functional *in vivo* (ref. 16, and below). We detected purified complexes by silver staining and total protein mixtures were analysed by liquid chromatography coupled with tandem mass spectrometry (LC–MS/MS). Negative controls were untagged cells. Purification of Lrs4 and Csm1 yielded peptides of INM proteins Heh1 (helix extension helix 1, also called Src1) and Nur1 (nuclear rim 1, Ydl089w) (Fig. 1c, d, and Supplementary Table 1, part A)[16]. Heh1, the orthologue of human Man1, is a member of a family of INM proteins containing a highly conserved LAP–Emerin–Man1 domain (LEM, also called HEH; Supplementary Fig. 2)[20–22]. LEM-domain proteins are linked to multiple clinical conditions through emerging roles in fundamental cellular processes, including gene expression and chromatin organization[6,7,20,21,23,24]. Little is known about Heh1 and Nur1 (ref. 20), which we define here as chromosome linkage INM proteins (CLIP). Purification of either INM protein yielded peptides for both Heh1 and Nur1 (Fig. 1e, f, and Supplementary Information, section A). Purification of Heh2, an Heh1 homologue (Supplementary Fig. 2)[20], did not yield peptides for CLIP or Cohibin proteins (Fig. 1e, f, Supplementary Fig. 3c and Supplementary Table 1). Moreover, TAP-tagged Heh1, Lrs4 and Csm1 immunoprecipitated together with Myc13-tagged Lrs4, Heh1 and Nur1, respectively (Supplementary Fig. 3d). Migration of Heh1 to 115 kDa, instead of the predicted 95 kDa, led us to identify multiple post-translational modifications of the protein and fluctuation of Heh1 levels over the cell cycle with peaks at interphase and mitosis (Supplementary Figs 3a, e, f and 4). These findings physically link rDNA-associated complexes to INM proteins.

Peripheral association of genes is linked to silent chromatin assembly, which seemingly stabilizes repeats by limiting access to recombination proteins[2,7]. Thus, CLIP may assemble at IGS1 to cooperate with RENT and Cohibin to silence transcription and inhibit unequal rDNA recombination. We therefore monitored unequal sister-chromatid exchange (USCE) by measuring the rate of loss of an *ADE2* marker gene from rDNA repeats. Deletion of Sir2, Lrs4 or Csm1 increased USCE, as expected (Fig. 2a, b, and Supplementary Table 4)[16,25]. USCE also increased after deletion of Heh1 or Nur1, but not of Heh2 (Fig. 2a, b, and Supplementary Table 4). *heh1Δ nur1Δ* cells showed additive USCE defects compared to single mutants, suggesting that INM proteins have partly overlapping functions at rDNA. Moreover, deletion of Heh1, Lrs4 or Csm1 exacerbated the effect of losing Sir2 (Fig. 2a and Supplementary Table 4)[16], suggesting that Sir2 stabilizes rDNA by means of processes that are both dependent on and independent of CLIP/Cohibin. Because increases in USCE affect rDNA copy number on Chr. XII, we analysed its size by using a contour-clamped homogeneous electric field (CHEF). Chr. XII measured about 2.83 megabase pairs in wild-type cells (about 190 rDNA units), and chromosome smearing in *sir2Δ* cells was indicative of

[1]Howard Hughes Medical Institute and [2]Department of Cell Biology, Harvard Medical School, Boston, Massachusetts 02115, USA.

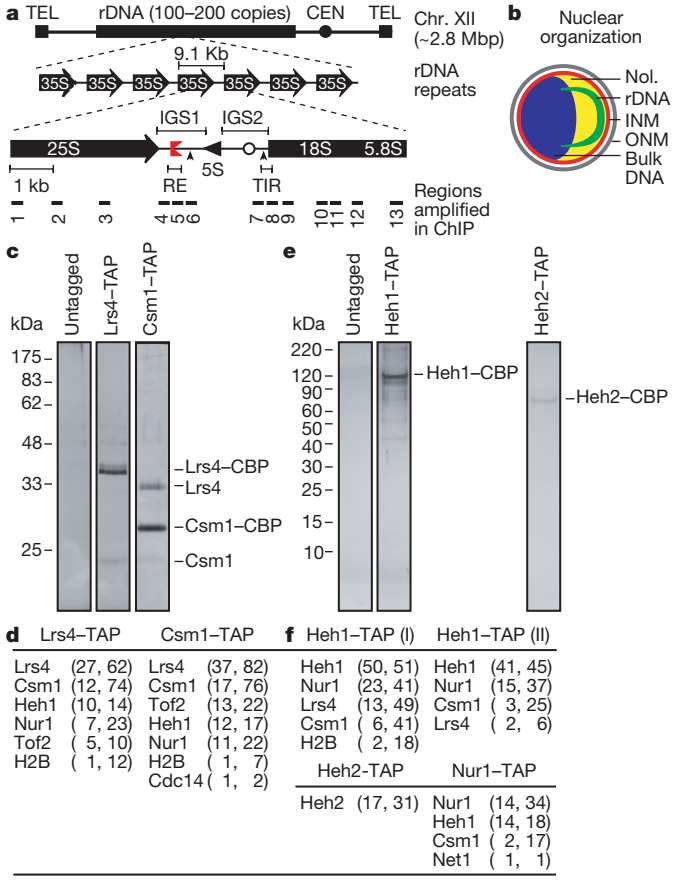

Figure 1 | Protein network extending from rDNA to the nuclear envelope. **a**, rDNA repeats on Chr. XII. Each unit yields a Pol I-transcribed 35S precursor rRNA (processed into 25S, 18S and 5.8S moieties) and a Pol III-transcribed 5S rRNA. CEN, centromere; TEL, telomere; IGS, intergenic spacer; RE, recombination enhancer; red symbol, replication fork block; TIR, Pol I transcription initiation region; open circle, DNA replication origin; Mbp, megabase pairs. Vertical arrowheads indicate insertion sites of *mURA3* reporter genes used in this study. **b**, Nuclear organization at the G_2/M cell-cycle stage. Nol., nucleolus; ONM, outer nuclear membrane. **c**–**f**, Purification of native complexes. **c**, **e**, Protein detection in silver-stained gels. TAP cleavage during protein purification leaves a calmodulin-binding protein (CBP) fragment. Results for purifications of Cohibin subunits (**c**) and INM proteins (**e**) are shown. **d**, **f**, LC–MS/MS analysis. Number of unique peptides followed by percentage coverage of the protein sequence is shown. Results for purifications of Cohibin subunits (**d**) and INM proteins (**f**) are shown. Full protein lists are given in Supplementary Table 1, part A, and spectral counts in Supplementary Tables 2 and 3.

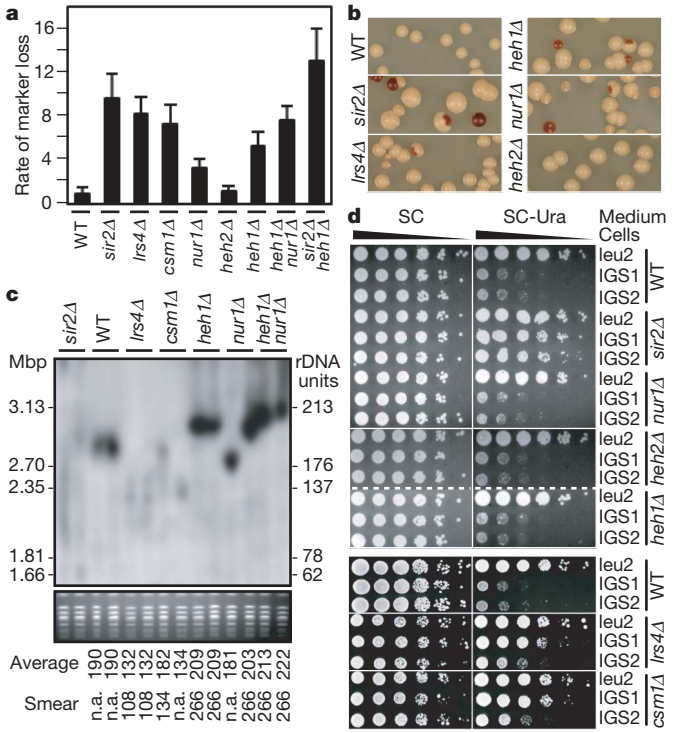

Figure 2 | Role of perinuclear protein network at rDNA repeats. **a**, **b**, Rates of *ADE2* marker loss (means ± s.d.) relative to wild-type (WT) (**a**) and representative colonies (**b**) are shown. **c**, CHEF analysis of rDNA stability. Top: chromosomes resolved by CHEF were probed with IGS1 rDNA (Chr. XII). Bottom: ethidium bromide (EtBr) staining of Chr. IV and smaller chromosomes shows the quality of the preparation. Values corresponding to rDNA copy number averages and smear edges are indicated. Chr. XII size for *sir2Δ* was too heterogeneous for copy number to be estimated. **d**, Unlike Sir2 and Cohibin, CLIP is dispensable for rDNA silencing. Tenfold serial dilutions of cells with the *mURA3* reporter gene inserted at IGS1/IGS2 (see Fig. 1a for locations) or outside rDNA at the *LEU2* locus are shown.

severe changes in rDNA copy number (Fig. 2c and Supplementary Fig. 5a), as expected[4,17]. Deletion of Lrs4, Csm1, Heh1 or Nur1 resulted in marked changes in rDNA copy-number averages and chromosome smearing patterns (Fig. 2c; described in Supplementary Information, section B). Together, these data suggest that the perinuclear protein network studied here is required for rDNA repeat stability.

We next studied the ability of cells to silence a Pol II-transcribed *mURA3* reporter gene positioned within IGS1 or IGS2 by assessing cellular growth on synthetic complete (SC) medium that either lacked uracil (−Ura; silencing disrupts growth) or was supplemented with 5-fluoro-orotic acid (+5FOA; silencing allows growth). Deletion of Sir2, Lrs4 or Csm1 disrupted IGS1 silencing (Fig. 2d), as expected[16]. However, in contrast to rDNA repeat stability, Heh1 and Nur1 were dispensable for silencing (Fig. 2d and Supplementary Fig. 5b), suggesting that silencing is insufficient for proper repeat-size regulation.

We next examined whether tethering rDNA repeats to INM proteins by means of Cohibin might limit recombination independently of silencing. Using immunofluorescence, we detected the functional green fluorescent protein (GFP)-tagged Net1 and Myc13-tagged Heh1 (Supplementary Table 4)[3,16]. Net1 associates with rDNA in the nucleolus throughout the cell cycle and recruits Sir2 to IGS1 (ref. 3). However, enrichment of Sir2 at rDNA in chromatin immunoprecipitation (ChIP) experiments is unaffected by deletion of Cohibin (Supplementary Figs 1 and 8c). To measure the limit of Net1–GFP internalization, the nucleus, delineated by peripheral Heh1–Myc13 signal, was divided into three concentric zones of equal area, zone I being the most peripheral[26]. Cells were categorized according to whether the centre of the least peripheral Net1–GFP focus localized to zone I, II or III. Most wild-type cells showed peripheral Net1–GFP localization (zone I, 74%), and few contained central Net1–GFP staining (zone III, 2%) (Supplementary Fig. 6a). Deletion of Lrs4 or Csm1 drastically shifted Net1–GFP to zone II or III (Supplementary Fig. 6a) and expanded the volume occupied by Net1–GFP within nuclear space in three dimensions (Fig. 3a), suggesting that optimal perinuclear localization of the rDNA-associated Net1 requires Cohibin.

How rDNA is separated from the bulk of nuclear DNA is unknown (Fig. 1b). We tested whether the perinuclear network studied here affects this subnuclear separation. Nocodazole-arrested cells were analysed by fluorescence *in situ* hybridization (FISH) to reveal rDNA, and 4,6-diamidino-2-phenylindole dihydrochloride (DAPI) staining to reveal bulk nuclear DNA. Wild-type cells showed line-shaped rDNA spooling away from the DNA bulk towards the nuclear periphery (Fig. 3b; quantified in Supplementary Fig. 6b)[27]. Deletion of Lrs4, Csm1 or Heh1, but not Heh2, caused rDNA to adopt amorphous distributions often overlapping the DAPI signal, and a small percentage of cells showed two separable rDNA bodies (Fig. 3b

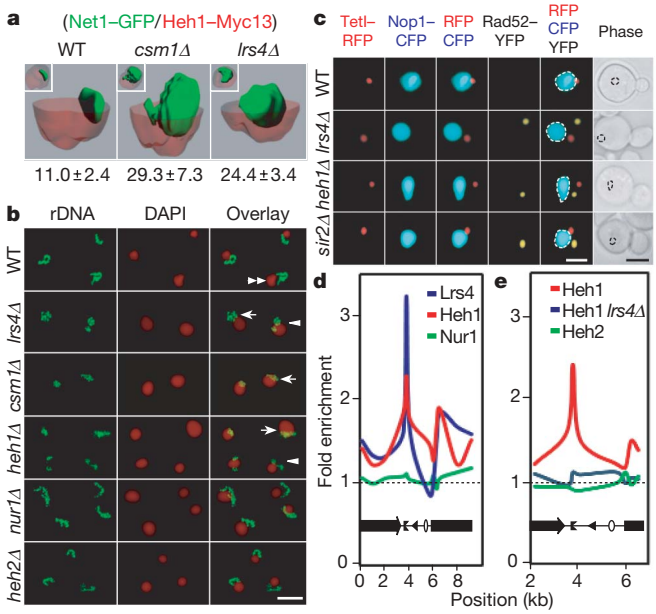

Figure 3 | Protein network tethers rDNA to the nuclear envelope. **a**, Representative three-dimensional reconstructions of cells from double immunofluorescence analysis reveal the relative organization of Net1–GFP (green) and Heh1-Myc13 (red). Signal boundaries are shown with clipping planes for Heh1–Myc13. Percentages of green relative to full red volumes are shown (means ± s.d.; $n = 5$). **b**, Nocodazole-arrested (G_2/M) cells were subjected to FISH to reveal rDNA and DAPI staining (pseudocoloured red) to detect bulk nuclear DNA. Cells with different rDNA morphologies are indicated by double arrowheads (spooled lines), arrows (amorphous) or triangles (two bodies) with quantifications in Supplementary Fig. 6b. Scale bar, 3 μm. **c**, Live cells with TetI–RFP-marked rDNA and expressing Rad52–YFP and nucleolar Nop1–CFP were imaged. Images depicting most observed phenotypes are shown. More images and quantifications are in Supplementary Fig. 6d–f. Scale bars, 1 μm (white) and 3 μm (black). **d**, **e**, Relative fold enrichment of indicated TAP-tagged proteins are shown. rDNA organization schematics are shown on graphs. kb, kilobases. Gels for **d** and **e** are shown in Supplementary Fig. 7a and Supplementary Fig. 7d, respectively. Detailed IGS1 ChIP is shown in Supplementary Fig. 7b, c.

and Supplementary Fig. 6b), which may have reflected a severe loss of interactions between rDNA repeats on Chr. XII sister chromatids. Deletion of Nur1 caused smaller changes in rDNA morphology, which appeared less condensed (Fig. 3b; 65 ± 6% of cells (mean ± s.d.)). Disorganization of rDNA was also observed in asynchronous cells (Supplementary Fig. 6c).

We next studied the localization of a specific site within rDNA repeats in live cells harbouring a *tetO* array at rDNA repeats and expressing *tetO*-binding TetI–RFP (TetI fused to red fluorescent protein) and the nucleolar Nop1–CFP (Nop1 protein fused to cyan fluorescent protein)[28]. TetI–RFP localized inside or at the periphery of the nucleolus in most wild-type cells (93%; Fig. 3c and Supplementary Fig. 6d, e). Deletion of Lrs4 or Heh1 shifted TetI–RFP outside the nucleolus or to its periphery (Fig. 3c and Supplementary Fig. 6d, e). *sir2Δ* cells showed less severe mislocalization of TetI–RFP (Fig. 3c and Supplementary Fig. 6d, e). Deletion of Lrs4, Heh1 or Sir2 also induced the formation of extranucleolar DNA repair centres, as marked by clustering of the yellow fluorescent protein (YFP)-tagged Rad52 recombination protein Rad52–YFP (Fig. 3c and Supplementary Fig. 6d, f). Fewer *sir2Δ* cells showed Rad52 foci than did *heh1Δ* or *lrs4Δ* cells (Supplementary Fig. 6f). This is in contrast to USCE in *sir2Δ* cells, which is higher than that in *heh1Δ* or *lrs4Δ* cells (Fig. 2a), suggesting that more recombinations in *sir2Δ* cells are unequal crossovers. Alternatively, a higher incidence of Rad52–YFP foci in cells lacking Heh1 or Lrs4 might suggest that these proteins stabilize several genetic loci. Most Rad52–YFP foci (61–65%) did not overlap TetI–RFP signal in *lrs4Δ*, *heh1Δ* or *sir2Δ* cells (Fig. 3c and Supplementary Fig. 6d, f), probably reflecting the occurrence of one or few repair events per rDNA array and their distance from *tetO* sequences. Although we cannot exclude the possibility that the *tetO* array contributes to rDNA mislocalization in *lrs4Δ*, *heh1Δ* or *sir2Δ* cells, disruption of rDNA organization in *lrs4Δ* and *heh1Δ* cells lacking *tetO* sites, as revealed by FISH and immunofluorescence (Fig. 3a, b, and Supplementary Fig. 6a–c), argues against this possibility and suggests that the perinuclear complexes studied here help to stabilize wild-type rDNA repeats. Together, these results suggest that Heh1 and Lrs4, and to a smaller extent Sir2, are required for the sequestration of rDNA in the peripherally located nucleolus, and show that loss of sequestration is correlated with increased repeat instability (Fig. 2) and Rad52 recombination foci.

To further analyse CLIP–Cohibin links, we performed ChIP with a combination of dimethyl adipimidate and formaldehyde crosslinkers. We observed 2.85 ± 0.37-fold and 2.35 ± 0.12-fold enrichments for IGS1 sequences in Lrs4–TAP and Heh1–TAP immunoprecipitations, respectively (Fig. 3d, e, and Supplementary Fig. 7). We did not detect an enrichment by using Nur1–TAP, probably due to its low abundance or weaker association with Cohibin (Fig. 3d and Supplementary Figs 3a and 7a–c). More significantly, deletion of Lrs4 abolished the IGS1 enrichment of Heh1–TAP without affecting its levels (Fig. 3e and Supplementary Fig. 7d–f). In contrast, no enrichment was detected for Heh2–TAP (Fig. 3e and Supplementary Fig. 7d), an INM protein that neither interacts with Cohibin (Fig. 1) nor affects rDNA stability (Fig. 2), although it is expressed to similar levels as Heh1 (data not shown)[29]. Together, these data indicate that CLIP–Cohibin-mediated tethering of rDNA repeats to the INM is required for repeat stability.

To determine whether perinuclear tethering suppresses recombination in the absence of Cohibin proteins, which are required for rDNA silencing and suppression of recombination, we created a strain in which rDNA was linked to Heh1 through Sir2. We fused *HEH1* and *SIR2* genes in *lrs4Δ* cells, creating a hybrid *HEH1–SIR2* gene (Fig. 4a). This yielded a fusion protein of the expected size (about 175 kDa) that was detectable by anti-Sir2 immunoblotting (Supplementary Fig. 8a). Fusion of Heh1 and Sir2 restored the separation of rDNA from bulk nuclear DNA in *lrs4Δ* cells (Fig. 4b), decreased unequal recombination (Fig. 4c and Supplementary Table 4) and increased homogeneity in the size of Chr. XII in cell populations (Fig. 4d and Supplementary Fig. 8b). Furthermore, ChIP revealed that Heh1–Sir2 became associated with rDNA at levels similar to those of Sir2 (Supplementary Fig. 8c). Moreover, Heh1–Sir2 did not rescue IGS1-specific increases in histone H3 acetylation, a marker for loss of silencing, caused by the deletion of Lrs4 (Supplementary Fig. 8c). The inability of Heh1–Sir2 to restore rDNA stability fully may be due to other Lrs4 functions, such as silencing or perhaps chromosome condensation, which suppress recombination at repeats. Attempts to fuse Heh1 with other perinuclear proteins, such as Tof2 or Ku70, did not yield viable cells (data not shown). Thus, tethering rDNA to the INM can promote repeat stability, at least partly independently of silencing.

Our results suggest that Sir2-dependent silencing alone cannot inhibit recombination within the repetitive rDNA locus and that INM-mediated perinuclear chromosome tethering ensures repeat stability (Fig. 4e and Supplementary Fig. 1). Extranucleolar Rad52 focus formation in *lrs4Δ*, *heh1Δ* or *sir2Δ* cells concurs with suggestions that although early rDNA recombination steps occur inside the nucleolus, Rad52 sumoylation and a high local concentration of the Smc5–Smc6 complex preclude Rad52 focus formation within nucleolar space[28]. Thus, our findings suggest that rDNA repeats unleashed from the INM accumulate lesions that can better access the nucleoplasm, in which high concentrations of functional Rad52 promote DNA repair by homologous recombination. Therefore, perinuclear tethering probably sequesters repeats from recombination factors and may be required for Cohibin and RENT to align rDNA sister chromatids stably during replication to prevent unequal

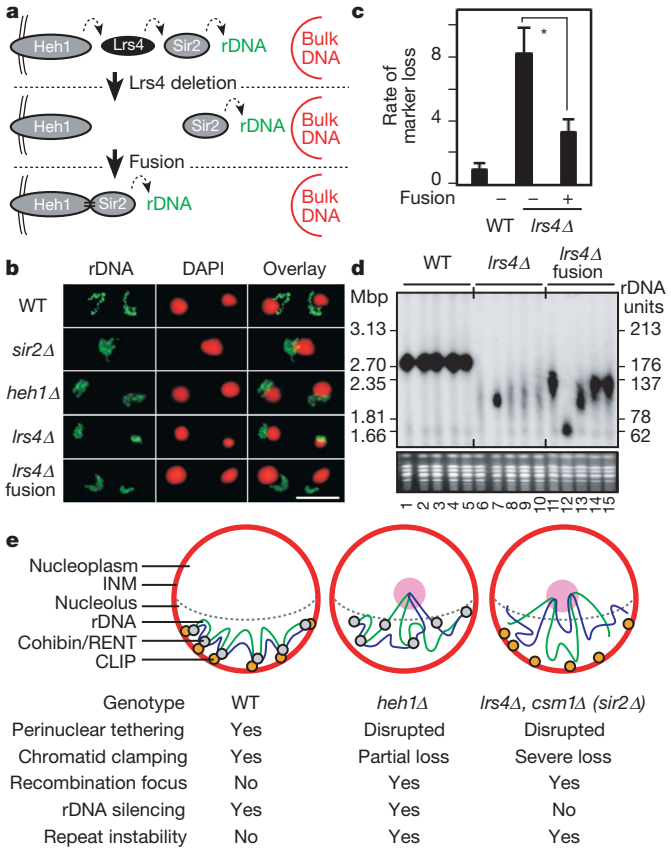

Genotype	WT	*heh1Δ*	*lrs4Δ, csm1Δ (sir2Δ)*
Perinuclear tethering	Yes	Disrupted	Disrupted
Chromatid clamping	Yes	Partial loss	Severe loss
Recombination focus	No	Yes	Yes
rDNA silencing	Yes	Yes	No
Repeat instability	No	Yes	Yes

Figure 4 | Targeted perinuclear tethering promotes rDNA repeat stability. **a**, Fusion of Heh1 to Sir2 in *lrs4Δ* cells. Heh1 is shown embedded in the INM. **b**, FISH reveals that fusion of Heh1 and Sir2 restores the separation of rDNA signal from DAPI staining in nocodazole-arrested cells lacking Lrs4. Scale bar, 3 μm. **c**, Relative rates of *ADE2* marker loss (means ± s.d.). Asterisk, $P < 0.0001$ for Student's *t*-test. **d**, CHEF analysis of rDNA stability. Top: chromosomes resolved by CHEF were probed with IGS1 rDNA (Chr. XII). Bottom: EtBr staining of Chr. IV and smaller chromosomes shows the quality of the preparation. **e**, Functional organization of the perinuclear molecular network tethering rDNA to the nuclear periphery. Repeat instability results from the loss of either the INM CLIP proteins or rDNA silencing complexes.

crossovers (Fig. 4e). Recombination between homologous repeats dispersed in the genome often instigates catastrophic chromosomal rearrangements. We expect that proteins studied here are members of perinuclear networks that control recombination at multiple loci to maintain genome stability.

METHODS SUMMARY

Standard co-immunoprecipitations[3,14], ChIP[14], TAP purification[16], immunofluorescence[16], rDNA silencing[16], USCE[16], FISH[27] and live-cell[28] assays were performed as described previously.

Full Methods and any associated references are available in the online version of the paper at www.nature.com/nature.

Received 11 July; accepted 26 September 2008.
Published online 9 November 2008.

1. Szostak, J. W. & Wu, R. Unequal crossing over in the ribosomal DNA of *Saccharomyces cerevisiae*. *Nature* **284,** 426–430 (1980).
2. Moazed, D. Common themes in mechanisms of gene silencing. *Mol. Cell* **8,** 489–498 (2001).
3. Straight, A. F. *et al.* Net1, a Sir2-associated nucleolar protein required for rDNA silencing and nucleolar integrity. *Cell* **97,** 245–256 (1999).
4. Bryk, M. *et al.* Transcriptional silencing of Ty1 elements in the RDN1 locus of yeast. *Genes Dev.* **11,** 255–269 (1997).
5. Smith, J. S. & Boeke, J. D. An unusual form of transcriptional silencing in yeast ribosomal DNA. *Genes Dev.* **11,** 241–254 (1997).
6. Capell, B. C. & Collins, F. S. Human laminopathies: nuclei gone genetically awry. *Nature Rev. Genet.* **7,** 940–952 (2006).
7. Reddy, K. L., Zullo, J. M., Bertolino, E. & Singh, H. Transcriptional repression mediated by repositioning of genes to the nuclear lamina. *Nature* **452,** 243–247 (2008).
8. Nomura, M. Ribosomal RNA genes, RNA polymerases, nucleolar structures, and synthesis of rRNA in the yeast *Saccharomyces cerevisiae*. *Cold Spring Harb. Symp. Quant. Biol.* **66,** 555–565 (2001).
9. Keil, R. L. & Roeder, G. S. *Cis*-acting, recombination-stimulating activity in a fragment of the ribosomal DNA of *S. cerevisiae*. *Cell* **39,** 377–386 (1984).
10. Brewer, B. J. & Fangman, W. L. A replication fork barrier at the 3′ end of yeast ribosomal RNA genes. *Cell* **55,** 637–643 (1988).
11. Kobayashi, T. & Ganley, A. R. Recombination regulation by transcription-induced cohesin dissociation in rDNA repeats. *Science* **309,** 1581–1584 (2005).
12. Visintin, R., Hwang, E. S. & Amon, A. Cfi1 prevents premature exit from mitosis by anchoring Cdc14 phosphatase in the nucleolus. *Nature* **398,** 818–823 (1999).
13. Shou, W. *et al.* Exit from mitosis is triggered by Tem1-dependent release of the protein phosphatase Cdc14 from nucleolar RENT complex. *Cell* **97,** 233–244 (1999).
14. Huang, J. & Moazed, D. Association of the RENT complex with nontranscribed and coding regions of rDNA and a regional requirement for the replication fork block protein Fob1 in rDNA silencing. *Genes Dev.* **17,** 2162–2176 (2003).
15. Rabitsch, K. P. *et al.* Kinetochore recruitment of two nucleolar proteins is required for homolog segregation in meiosis I. *Dev. Cell* **4,** 535–548 (2003).
16. Huang, J. *et al.* Inhibition of homologous recombination by a cohesin-associated clamp complex recruited to the rDNA recombination enhancer. *Genes Dev.* **20,** 2887–2901 (2006).
17. Gottlieb, S. & Esposito, R. E. A new role for a yeast transcriptional silencer gene, SIR2, in regulation of recombination in ribosomal DNA. *Cell* **56,** 771–776 (1989).
18. Fritze, C. E., Verschueren, K., Strich, R. & Easton Esposito, R. Direct evidence for SIR2 modulation of chromatin structure in yeast rDNA. *EMBO J.* **16,** 6495–6509 (1997).
19. Smith, J. S., Caputo, E. & Boeke, J. D. A genetic screen for ribosomal DNA silencing defects identifies multiple DNA replication and chromatin-modulating factors. *Mol. Cell. Biol.* **19,** 3184–3197 (1999).
20. King, M. C., Lusk, C. P. & Blobel, G. Karyopherin-mediated import of integral inner nuclear membrane proteins. *Nature* **442,** 1003–1007 (2006).
21. Brachner, A., Reipert, S., Foisner, R. & Gotzmann, J. LEM2 is a novel MAN1-related inner nuclear membrane protein associated with A-type lamins. *J. Cell Sci.* **118,** 5797–5810 (2005).
22. Rodriguez-Navarro, S., Igual, J. C. & Perez-Ortin, J. E. SRC1: an intron-containing yeast gene involved in sister chromatid segregation. *Yeast* **19,** 43–54 (2002).
23. Hellemans, J. *et al.* Loss-of-function mutations in LEMD3 result in osteopoikilosis, Buschke–Ollendorff syndrome and melorheostosis. *Nature Genet.* **36,** 1213–1218 (2004).
24. Bione, S. *et al.* Identification of a novel X-linked gene responsible for Emery–Dreifuss muscular dystrophy. *Nature Genet.* **8,** 323–327 (1994).
25. Kaeberlein, M., McVey, M. & Guarente, L. The SIR2/3/4 complex and SIR2 alone promote longevity in *Saccharomyces cerevisiae* by two different mechanisms. *Genes Dev.* **13,** 2570–2580 (1999).
26. Gartenberg, M. R., Neumann, F. R., Laroche, T., Blaszczyk, M. & Gasser, S. M. Sir-mediated repression can occur independently of chromosomal and subnuclear contexts. *Cell* **119,** 955–967 (2004).
27. Guacci, V., Hogan, E. & Koshland, D. Chromosome condensation and sister chromatid pairing in budding yeast. *J. Cell Biol.* **125,** 517–530 (1994).
28. Torres-Rosell, J. *et al.* The Smc5–Smc6 complex and SUMO modification of Rad52 regulates recombinational repair at the ribosomal gene locus. *Nature Cell Biol.* **9,** 923–931 (2007).
29. Ghaemmaghami, S. *et al.* Global analysis of protein expression in yeast. *Nature* **425,** 737–741 (2003).

Supplementary Information is linked to the online version of the paper at www.nature.com/nature.

Acknowledgements We thank C. Yip, T. Walz, J. Huang, M. Bühler, D. Koshland, A. Palazzo, D. E. Libuda, F. Winston, L. Vasiljeva, S. Buratowski, J. E. Warner, C. Anderson, G. A. Beltz, M. Lisby, T. Daniel, L. Ding and the Harvard NeuroDiscovery Optical Imaging Center for technical assistance or materials, and T. Rapoport, T. Iida, M. Motamedi, A. Johnson, M. Onishi, E. Gerace, S. Buker, M. Halic and members of the Moazed laboratory for helpful discussions and comments. This work was supported by the National Institutes of Health and the Howard Hughes Medical Institute (D.M.), and the Canadian Institutes of Health Research Institute of Aging (K.M.). D.M. is a scholar of the Leukemia and Lymphoma Society.

Author Contributions K.M. and D.M. designed experiments and wrote the paper. K.M. and J.S. performed LC–MS/MS analyses. K.M. performed the other experiments. S.P.G. provided mass spectrometry expertise and equipment.

Author Information Reprints and permissions information is available at www.nature.com/reprints. Correspondence and requests for materials should be addressed to D.M. (danesh@hms.harvard.edu).

METHODS

Strains and materials. Endogenous genes were deleted or modified with carboxy-terminal epitope tags as described[14,16]. Strains harbouring *mURA3* reporter genes were described[14]. For Heh1–Sir2 fusion, *HEH1* was amplified with its promoter from genomic DNA with primers KM11 (5′-GATAactagtTTCTGCCTGTAGAGAGAG-3′) and KM12 (5′-GATAgggcccCAAATATGGCAACTCGGA-3′). *Spe*I–*Apa*I-digested products were ligated into pRS314, yielding a plasmid used as a template to amplify *HEH1* with the upstream *TRP1* gene with primers KM14 (5′-CATTCAAACCATTTTTCCCTCATCGGCACATTAAAGCTGGATGTCTGTTATTAATTTCAC-3′) and KM17 (5′-CGCTAGTCTTTGATACGGCGTATTTCATATGTGGGATGGTTATTTTGTTTTCAGCGGAAT-3′) adding regions flanking endogenous *SIR2* start site. Cells lacking the endogenous *HEH1* open reading frame, transformed with PCR products and selected on −TRP medium were PCR/immunoblotting-screened. Antibodies: anti-Myc-9E10 (Covance), anti-actin (Millipore), HRP-conjugated anti-TAP or anti-Myc (Invitrogen), anti-digoxin (Jackson Laboratories), anti-AcK9/AcK14 H3 (Millipore), anti-CBP (Open Biosystems), anti-cyclin-B2 and anti-GFP (A. Rudner), Rhodamine-tagged goat anti-mouse (Jackson Laboratories), Alexa488-labelled goat anti-rabbit (Molecular Probes), FITC-conjugated goat anti-mouse (Jackson Laboratories), FITC-conjugated swine anti-goat (Invitrogen), anti-Sir2 (ref. 30).

Protein purifications. Standard assays were performed as described[16]. Purifications incorporating CHAPS were performed as described[16] with modifications: (1) 1% CHAPS was added to lysis and TEV-cleavage buffers. (2) CHAPS (0.05%) was added to CAM binding and elution buffers. (3) Regarding purified mixtures, 10–50% was subjected to electrophoresis/silver staining and half was precipitated with trichloroacetic acid for spectrometric analysis.

Mass spectrometry.. Trypsin-digested mixtures were subjected to LC–MS/MS[31] and MS/MS spectral analysis[32] as described (less than 1% false positive rate). Proteins in untagged controls were removed. Spectral counts semiquantitatively measuring the relative abundance of proteins are given in Supplementary Tables 2 and 3. Excised gel bands were minced, destained, dehydrated and trypsin-digested before extraction of digests. Modifications were identified with SEQUEST Sorcerer (Sage-N Research) allowing variable methionine oxidation, serine/threonine phosphorylation and lysine ubiquitylation. Only unambiguous phosphosites[33] are reported.

FISH. Experiments were conducted as described[27]. rDNA probes were a gift from V. Guacci or were prepared from *Bgl*II fragments from plasmids p362 and p363, which contain the 5′ and 3′ halves of an rDNA unit, respectively, using the BioNick (Invitrogen) and digoxigenin (Roche) labelling systems[27]. Scoring was conducted at the microscope; representative images adjusted for contrast and colouring are shown.

Imaging. Images were collected with an Axiovert 200 microscope (Carl Zeiss) coupled to an EM–charge-coupled device digital camera (Hamamatsu Photonics) or an Eclipse 80i microscope (Nikon). The positions of GFP spots were determined as described[26]. The outer circle was set to coordinates at which the red signal shows the largest decrease in intensity, moving centrally, as revealed by ImageJ (National Institutes of Health). Scoring and measurements were conducted with Metamorph (Molecular Devices) and representative images were adjusted for background using levels and contrast in Photoshop (Adobe). Other software programs handling data were Office (Microsoft) and FreeHand (Macromedia).

Three-dimensional reconstruction. An average of four images for each of about 15 *Z* sections were generated with a Zeiss LSM510 (Carl Zeiss) upright confocal microscope (Harvard NeuroDiscovery Optical Imaging Center). Respective settings for red and green signals were LP-560 and LP-505 emission, 543 and 488 nm excitation, 50 and 62 μm pinhole. Constant background corrections were performed in ImageJ. Reconstruction was performed with volume tools of Imaris (Bitplane).

ChIP. Standard ChIP (Supplementary Fig. 8) was conducted as described[14]. Modified ChIP (Fig. 3 and Supplementary Fig. 7) was conducted as described[14,16] with protein–protein crosslinkers added[34]. Modifications are as follows. Yeast cultures (50 ml) were grown to $D_{600} \approx 0.8$. Cells were centrifuged, washed with ice-cold PBS, suspended in 10 ml of ice-cold fresh protein–protein crosslinking solution (10 mM dimethyl adipimidate, 0.25% dimethyl sulphoxide in PBS) and nutated at room temperature (22–24 °C) for 45 min. PBS-washed cells were resuspended in 50 ml of 1% formaldehyde in PBS for 11 h, then glycine was added to 125 mM. PBS-washed cells were resuspended in 400 μl of lysis buffer and subjected to bead-beating; procedures were continued as described[14,16] except that RNase was added before proteinase K. Dilutions for immunoprecipitation and input DNA were 1:2 and 1:20,000, respectively. [α-^{32}P]dCTP-labelled and EtBr-stained products were quantified with Molecular Imager/QuantityOne (Bio-Rad) and Image ReaderLAS-3000/ImageGauge (Fuji), respectively.

USCE. Assays were performed essentially as described[16,25]. Cells were grown to $D_{600} = 0.4–0.8$, sonicated briefly, and spread (about 400 cells per plate) on thick plates (5 mg l^{-1} adenine). Incubation was at 30 °C for 5 days, at 4 °C for 2 days, then at room temperature for 3 days. Rates were obtained by dividing the number of half-sectored colonies by the total number of colonies excluding completely red colonies.

CHEF and Southern blotting. Experiments were conducted as described[11,35,36], with modifications. Saturated overnight culture (1 ml) was washed and suspended in 300 μl of EDTA/Tris (50 mM EDTA, 10 mM Tris-HCl pH 7.5). Zymolyase (2 μl; 20 μg μl^{-1} in 10 mM Na_2HPO_4 pH 7.5) and 500 μl of low-melting-point CHEF-quality agarose (1% in 125 μM EDTA pH 8.0, 42 °C; Bio-Rad) were added and the mixture was solidified in plug moulds at 4 °C. Plugs were incubated overnight in 1 ml of 10 μM Tris-HCl pH 7.5, 500 μM EDTA at 37 °C, then overnight in 1 ml of 2 mg ml^{-1} proteinase K in 10 μM Tris-HCl pH 7.5, 500 μM EDTA, 10 mg ml^{-1} *N*-lauroylsarcosine at 50 °C. Plugs were washed three times with EDTA/Tris (4 °C, 1 h per wash) and stored in 2 ml of EDTA/Tris (4 °C). Plugs were prepared at $5 \times 3 \times 1.5$ mm^3 and run (68 h, 3.0 V cm^{-1}, 300–900 s, 10 °C) on a 0.8% CHEF agarose gel in 0.5 × TBE/CHEF-DR-II (Bio-Rad). CHEF size markers were *Hansenula wingei* chromosomes (Bio-Rad). EtBr-stained gels were imaged then subjected to standard Southern blotting. Blots were crosslinked by ultraviolet and probed (65 °C, 16 h) with [^{32}P]dCTP-labelled IGS1.

Whole cell protein preparation. Lysates were prepared by bead-beating[16] except for those shown in Supplementary Fig. 8a; the latter were prepared by trichloroacetic acid-coupled lysis because Heh1–Sir2 was otherwise unstable. For this, 2×10^7 cells grown to $D_{600} \approx 0.75$ were washed and suspended in 500 μl of ice-cold water. Sequential additions of 75 μl of alkali/2-mercaptoethanol (1.85 M NaOH, 1.065 M 2-mercaptoethanol) and 75 μl of 50% trichloroacetic acid solutions were each followed by a 10-min incubation on ice. After centrifugation (10,000 r.p.m. at 4 °C for 10 min), pellets were suspended in loading buffer (1 × standard loading buffer, 1.42 M 2-mercaptoethanol, 83.2 mM Tris-HCl pH 8.8) and boiled, and supernatants were saved.

α-Factor arrest. Cells grown to $D_{600} = 0.2$ were incubated for 3 h with α-factor (10 μg ml^{-1}). Cells were washed and resuspended in fresh medium; samples collected every 15 min were frozen in liquid nitrogen.

30. Moazed, D. & Johnson, D. A deubiquitinating enzyme interacts with SIR4 and regulates silencing in *S. cerevisiae*. *Cell* **86**, 667–677 (1996).
31. Haas, W. *et al.* Optimization and use of peptide mass measurement accuracy in shotgun proteomics. *Mol. Cell. Proteomics* **5**, 1326–1337 (2006).
32. Buker, S. M. *et al.* Two different Argonaute complexes are required for siRNA generation and heterochromatin assembly in fission yeast. *Nature Struct. Mol. Biol.* **14**, 200–207 (2007).
33. Beausoleil, S. A., Villen, J., Gerber, S. A., Rush, J. & Gygi, S. P. A probability-based approach for high-throughput protein phosphorylation analysis and site localization. *Nature Biotechnol.* **24**, 1285–1292 (2006).
34. Kurdistani, S. K. & Grunstein, M. *In vivo* protein–protein and protein–DNA crosslinking for genomewide binding microarray. *Methods* **31**, 90–95 (2003).
35. Oakes, M., Siddiqi, I., Vu, L., Aris, J. & Nomura, M. Transcription factor UAF, expansion and contraction of ribosomal DNA (rDNA) repeats, and RNA polymerase switch in transcription of yeast rDNA. *Mol. Cell. Biol.* **19**, 8559–8569 (1999).
36. Libuda, D. E. & Winston, F. Amplification of histone genes by circular chromosome formation in *Saccharomyces cerevisiae*. *Nature* **443**, 1003–1007 (2006).